

RME57C-25a

~~CONFIDENTIAL~~Copy 173  
RM E57G25a~~UNCLASSIFIED~~

# RESEARCH MEMORANDUM

PRELIMINARY INVESTIGATION OF SHIELD TO IMPROVE  
ANGLE-OF-ATTACK PERFORMANCE OF  
NACELLE-TYPE INLET

By Milton A. Beheim and Thomas G. Piercy

Lewis Flight Propulsion Laboratory  
Cleveland, Ohio

TECHNICAL LIBRARY  
AIRSEARCH MANUFACTURING CO.  
9851-9951 SEPULVEDA BLVD.  
LOS ANGELES 45  
CALIFORNIA

CLASSIFIED DOCUMENT

This material contains information affecting the National Defense of the United States within the meaning of the espionage laws, Title 18, U.S.C., Secs. 793 and 794, the transmission or revelation of which in any manner to an unauthorized person is prohibited by law.

NATIONAL ADVISORY COMMITTEE  
FOR AERONAUTICS

WASHINGTON

October 2, 1957

Classification	<del>CONFIDENTIAL</del>	UNCLASSIFIED
CHANGED TO	1-21-60	
By authority of		Mississ. Bul. #11
Changed by		BfC Date 6-26-75

~~CONFIDENTIAL~~~~UNCLASSIFIED~~

## NATIONAL ADVISORY COMMITTEE FOR AERONAUTICS

RESEARCH MEMORANDUMPRELIMINARY INVESTIGATION OF SHIELD TO IMPROVE ANGLE-OF-  
ATTACK PERFORMANCE OF NACELLE-TYPE INLET

By Milton A. Beheim and Thomas G. Piercy

## SUMMARY

An investigation was conducted at Mach numbers between 1.6 and 2.0 on the use of a shield along the upper-half periphery of the cowl of a conical inlet to improve performance at angle of attack. The best results were obtained with the shield mounted in such a manner that an air gap existed between the shield and the cowl lip. Zero-angle-of-attack performance was not appreciably affected. At an angle of attack of 8° distortion was about half that without the shield, and subcritical stability was improved.

## INTRODUCTION

The deleterious effects of angle of attack on the performance of nacelle-type supersonic diffusers is well known (e.g., ref. 1). Several investigations have been made of methods to reduce the sensitivity of this type of inlet. The object in the work of references 2 to 4 was primarily to maintain pressure recovery and mass flow over a range of angle of attack; however, it is now recognized that in many cases distortion and subcritical stability may be the more important performance parameters for this type of operation. Pivoting the cone to aline it with the free stream in the manner of reference 4 improved the subcritical stability for cowl-lip-position parameters greater than the conical shock angle of the centerbody. Canting the plane of the cowl lip as in the investigation of reference 5 improved several performance parameters at angle of attack, particularly distortion, but caused some deterioration of zero-angle-of-attack performance.

Another method of improving the angle-of-attack performance would be to shield the inlet so as to reduce the effective angle of attack. A brief investigation has been conducted at the NACA Lewis laboratory of an arrangement in which a semicircular shield is placed adjacent to and upstream of the upper half of the cowl lip; this study is the subject of the present report. Also included in this report is a comparison of the

subcritical stability and distortion of this and several other inlets designed for improved angle-of-attack performance. Some of these data were previously unpublished.

#### SYMBOLS

m mass-flow rate  
P total pressure  
 $\Delta$  maximum minus minimum  
 $\theta_l$  angle between inlet axis and line from cone apex to cowl lip  
 $\theta_s$  conical shock angle of centerbody

#### Subscripts:

l local  
0 conditions in free stream in maximum capture area of inlet  
2 conditions at diffuser exit (compressor face)

#### APPARATUS

Two models were investigated in two facilities: a full-scale model in the 8- by 6-foot wind tunnel at Mach numbers of 1.6, 1.8, and 2.0, and a small-scale model in the 18- by 18-inch tunnel at Mach 1.91. The geometry of the shields of the two inlets differed. Photographs of the two inlets appear in figure 1, and schematic sketches are presented in figure 2.

The small-scale inlet was the same as that investigated in reference 4 except for the shield added to the cowling. The design of the shield was arbitrary in that the tip was 0.65 of the cowl-lip radius upstream of the cowling and was adjacent to the cowling along the upper-half periphery. The inlet had a 25° half-angle conical centerbody, and the cowl-lip-position parameter was varied by translating the cowling. As described in reference 4, the conical portion of the centerbody could be pivoted and aligned with the free stream regardless of model angle of attack. Subsonic diffuser area variations are shown in figure 3(a).

The large-scale model is that identified as  $C_{14}S_b$  in reference 6. For this inlet the relative length of the shield was much greater. The tip of the shield was 2.54 times the cowl-lip radius upstream of the cowling and was adjacent to the cowling at only two points. Presumably the air gap between the shield and the cowling would aid in starting the inlet and also reduce the possibility of shock - boundary-layer interaction near the cowl lip by allowing the boundary layer from the shield to escape to the free stream. This inlet also had a  $25^\circ$  half-angle conical centerbody, and the cowl-lip-position parameter was varied by translating the conical portion of the centerbody. A flush-slot boundary-layer-bleed arrangement was located in the centerbody surface just inside the cowling. Subsonic diffuser area variations are shown in figure 3(b).

The Reynolds number based on cowl-lip diameter was  $7.1 \times 10^5$  for the small model and about  $7 \times 10^6$  for the large model.

## PROCEDURE

The small model was investigated at several angles of attack from zero to  $14^\circ$ , but the large model was tested only at zero and  $8^\circ$ . Mass flow was regulated with sonic plugs for both inlets and was computed from the sonic area and measured average total pressure at station 25.4 with the small inlet and from the sonic area and average static pressure at station 122.5 with the large model. An area-weighted average of the total-pressure measurements was used to obtain pressure recovery. A distortion parameter, defined as the maximum total pressure minus the minimum divided by the local average, was determined at the diffuser exits in a circular flow passage with the small inlet and in an annular flow passage with the large inlet (figs. 2(a) and (b)). Inlet buzz is defined as an operating condition for which any visible portion of the shock structure oscillated.

## RESULTS

### Large-Scale Model

The performance of the full-scale model without the shield from reference 6 is plotted in figure 4 for two values of  $\theta_7$  at a Mach number of 2 and angles of attack of zero and  $8^\circ$ . The effect of adding the shield at  $8^\circ$  is also shown. The performance of this inlet with the shield at zero angle of attack was not recorded at Mach 2, but check points computed during tunnel operation indicated this performance to be essentially the same as that without the shield. Zero-angle-of-attack performance at Mach numbers of 1.8 and 1.6 with and without the shield is compared in figure 5 for several values of  $\theta_7$ . The effect

of the shield varied depending upon Mach number and  $\theta_l$ . At Mach 1.8 (fig. 5(a)) the subcritical stability was decreased by the shield with the conical shock upstream of the cowl ( $\theta_l = 42.6^\circ$ ), but otherwise the performances were the same or even better. At Mach 1.6 (fig. 5(b)) the performances again differed with the conical shock upstream of the cowl ( $\theta_l = 46^\circ$ ). In particular, recovery was lower with the shield and distortion greater. With the conical shock at the cowl ( $\theta_l = 51^\circ$ ) the performances once more were nearly identical. No instability was observed at this Mach number.

At an angle of attack of  $8^\circ$  at Mach 2 (fig. 4), pressure recovery was appreciably lower with the shield, but distortion was reduced by half, and subcritical stability increased. The minimum stable mass-flow ratio was not determined but was less than the lowest values for which data are shown.

Distortion contours from this model at Mach 2 are shown in figure 6. In figures 6(a) and (b) critical operation without the shield at zero and  $8^\circ$  angles of attack is shown, and in figure 6(c) critical operation with the shield at the  $8^\circ$  angle of attack is shown. The low-energy region that later is shown to occur on the shield side of the inlet with the small model did not occur in this case, presumably because: (1) there was less opportunity for a shock - boundary-layer interaction to occur and (2) any air affected by such an interaction would not enter the inlet but could escape between the shield and the cowl.

The shock configurations at zero and  $8^\circ$  angles of attack for Mach 2 operation and  $\theta_l = 42.6^\circ$  with and without the shield are illustrated in figure 7. At zero angle there is little effect of the shield on the shock structure near the cowling (figs. 7(a) and (c)). In reference 5 the severe turning requirements at angle of attack in the region of the lower cowl lip with  $\theta_l = \theta_s$  for the conventional type of inlet are shown to be a source for high distortion. As shown in figure 7(d), the shield caused a strong oblique shock to form ahead of the lower cowl lip that was not present when the shield was removed (fig. 7(b)). This oblique shock would alleviate the high turning at the lower cowl lip and could account for the low distortion of this configuration near critical operation at angle of attack.

#### Small-Scale Model

The small-scale model was investigated a few years before the large-scale investigation, but results were not reported. The results obtained with the small-scale model were generally inferior to those with the large model, but because the small-model data were obtained over a larger range of mass-flow ratio and angle of attack, they are presented at this

time. In figure 8 the pressure-recovery - mass-flow characteristics of the inlet without the shield from reference 4 are plotted for two cowl-lip-position parameters. The conical shock angle was  $44^\circ$ . The distortion parameter is also shown. The unusually large amount of subcritical stability obtained with the oblique shock inside the cowling ( $\theta_l = 44.7$ , fig. 8(b)) at zero angle of attack was lost at angles of attack greater than  $1.5^\circ$  (data are not shown at this angle).

The performance of the same inlet with the shield in position is presented in figure 9 for the same values of the cowl-lip-position parameter. The inlet performance at zero angle of attack was adversely affected by the shield, particularly with  $\theta_l = 41.8^\circ$  (fig. 9(a)). With this value of  $\theta_l$  the normal shock was not swallowed in the region of the shield at any angle of attack. The normal shock was swallowed at zero angle of attack with  $\theta_l = 44.7^\circ$  (fig. 9(b)) but not at angles of attack greater than  $1.5^\circ$ . Subcritical stability was greatly increased by the presence of the shield. With  $\theta_l = 41.8^\circ$  much stability was obtained for angles of attack to about  $6^\circ$ , and with  $\theta_l = 44.7^\circ$  no instability was encountered at any angle of attack over the complete range in airflow except for slightly subcritical mass flows at zero angle of attack. For this condition the normal shock oscillated locally as it was passed in either direction over the shield. (As indicated earlier, this was the only configuration investigation for which the shock could be swallowed.) The critical pressure recovery at low angles of attack was decreased with the shield, but at angles of attack greater than about  $12^\circ$  it was slightly higher. Generally the shield caused large increases in distortion. Mach number contour maps in figure 10 for critical operation with and without the visor show a low-energy region on the shield side of the inlet with the shield in position, regardless of angle of attack, that was not present when the shield was removed. This probably was a result of shock interaction with the boundary layer from the shield.

Data are not presented, but pivoting the cone to aline it with the free stream in the manner of reference 1 with the visor in position improved the subcritical stability with  $\theta_l = 41.8^\circ$  at high angles of attack, and therefore the stability range remained large over the angle-of-attack range. With  $\theta_l = 44.7^\circ$  the stability decreased somewhat at angle of attack. Again distortions were large.

Schlieren and shadowgraph photographs for a variety of operating conditions with the shield in position are shown in figure 11. Figures 11(a) to (c) show operation at zero angle of attack. As shown in figure 11(a) the inlet did not start completely with  $\theta_l = 41.8^\circ$  but did start with  $\theta_l = 44.7^\circ$  (fig. 11(b)). The subcritical operating condition at which buzz just stopped with  $\theta_l = 44.7^\circ$  is shown in figure 11(c).

In figures 11(d) and (e) supercritical operation is shown at two angles of attack,  $3^\circ$  and  $14^\circ$ .

### Inlet Comparison

An inlet - turbojet-engine configuration operated over a range in angle of attack at constant flight Mach number and altitude would remain, in many installations, at constant corrected airflow (or diffuser-exit Mach number). To evaluate the performance for such operation of several inlets designed for improved angle-of-attack characteristics, a corrected airflow line was selected for each inlet that would yield near optimum thrust minus drag at zero angle of attack and would not enter an unstable operating condition over the angle-of-attack range investigated. This match line for the inlets discussed is shown on the pressure-recovery - mass-flow graphs of figures 4, 8, and 9. Other inlets considered are the pivoted-cone inlet of reference 4, the vertical-wedge cutback-cowl inlet of reference 2, and the pivoted-cone swept-cowl inlet of reference 5.

A summary of the distortion resulting from operation along this airflow line is presented in figure 12 for these inlets. Data for small-scale models at a Mach number of 1.91 appear in figure 12(a) and for the large-scale model at Mach 2 in figure 12(b).

Of the small-scale conventional conical inlets (i.e., conventional cowling, cone not pivoted) in figure 12(a), lower distortion was obtained with  $\theta_l = 41.8^\circ$  than with  $\theta_l = 44.7^\circ$ . As indicated in reference 5, the lower distortion with the lower  $\theta_l$  was a result of preturning of the air upstream of the cowl by the conical shock and also a result of the slightly lower diffuser-exit Mach number. Pivoting the cone to align it with the free stream with  $\theta_l = 41.8^\circ$  (but no shield) produced slight improvements in distortion. This configuration had the lowest distortion over most of the angle-of-attack range. Data are not presented, but pivoting the cone with  $\theta_l = 44.7^\circ$  caused appreciable increases in distortion.

The swept-cowl pivoted-cone inlet of reference 5 had a higher distortion at low angles of attack than the unswept-cowl inlet discussed here. At higher angles of attack (above  $5^\circ$ ) this swept-cowl inlet had a lower distortion than the unswept cowl with about the same  $\theta_l$  ( $44^\circ$  to  $44.7^\circ$ ), but the distortion was not as low as with the conventional cowl and  $\theta_l = 41.8^\circ$ . The swept cowl with the vertical-wedge compression surface had about the same distortion at small angles of attack as the swept-cowl conical inlet, but the distortion increased at a faster rate with angle of attack for the vertical wedge.

Adding the shield to the cowling caused large increases in distortion at moderate angles of attack for either value of  $\theta_l$  (data are shown only for  $\theta_l = 41.8^\circ$ ), but decreases in distortion at angles of attack greater than  $12^\circ$ . The lowest distortion at an angle of attack of  $14^\circ$  for the small-scale model was obtained with this configuration.

With the large-scale model (fig. 12(b)) distortion increased rapidly without the shield. With the shield the distortion was reduced by half at an angle of attack of  $8^\circ$ .

A stability margin, defined as the difference between the match mass-flow ratio as described earlier and the minimum stable mass-flow ratio, is summarized over the angle-of-attack range in figure 13 for the inlets discussed in figure 12. As shown in figure 13(a) the conventional conical inlet exhibited a decrease in stability margin with increasing angle of attack with either value of  $\theta_l$ , but particularly so with  $\theta_l = 44.7^\circ$ .

Pivoting the cone with  $\theta_l = 41.8^\circ$  caused the stability margin to remain constant as angle of attack varied; and although data are not shown for the cone pivoted and  $\theta_l = 44.7^\circ$  because of the high distortion, the stability margin remained large over the angle-of-attack range. Thus, pivoting the cone was beneficial in this respect.

The swept conical inlet (with  $\theta_l = 44^\circ$ ) also employed a pivoted cone, and its stability margin also remained fairly constant for all angles of attack. The swept-cowl vertical-wedge inlet had a somewhat greater stability margin at zero angle of attack than the swept-cowl conical inlet, but the stability margin decreased as angle of attack increased.

With the shield in position and  $\theta_l = 41.8^\circ$ , the stability margin was large for angles of attack less than  $6^\circ$  when the cone was not pivoted, and, although data are not shown, the stability margin was also large over the entire angle-of-attack range when the cone was pivoted. Data are not presented in this figure for  $\theta_l = 44.7^\circ$  with the shield; however, the stability margin was very large over the angle-of-attack range except for the minor disturbance at zero angle of attack.

The stability margin of the large unshielded model also decreased as angle of attack increased (fig. 13(b)). The use of the shield increased the stability margin, but the exact amount was not measured. In any case the increase was greater than the amount shown on the figure, as indicated by the arrows. Thus, although the data obtained with the large inlet were limited, it appears that a well designed shield such as that used with this inlet offers promise as a means to improve distortion and subcritical stability at angle of attack. The results with the small-scale model indicate the possibility that this increase in stability might be large.

## SUMMARY OF RESULTS

An investigation was conducted on the use of a shield upstream of the upper-half periphery of the cowl of a conical inlet to improve performance at angles of attack. Two arrangements were used: a small-scale model with a visor essentially an axial extension of a portion of the cowl lip, and a large-scale model with an air gap between the shield and the cowl lip. The relative length of the shield was greater with the large model than with the small model. The small-scale model was operated at angles of attack from zero to  $14^{\circ}$  at a Mach number of 1.91, and the cone could be pivoted to be alined with the free stream, if desired. The large-scale model was investigated at angles of attack of zero and  $8^{\circ}$  in the Mach number range from 1.6 to 2.0, and the cone could not be pivoted. The following results were obtained:

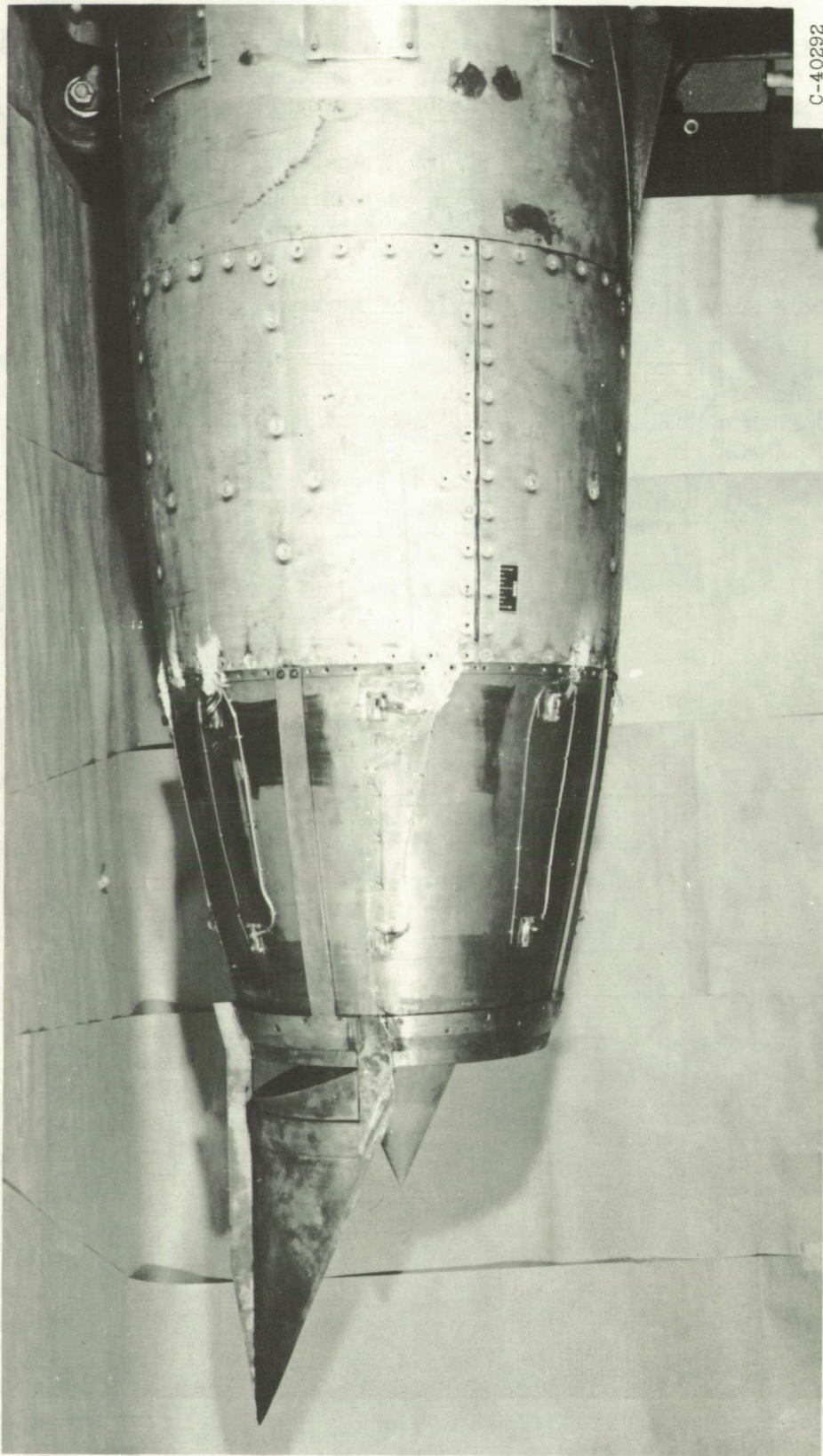
1. An air gap between the shield and the cowl, such as that with the large model, was necessary to maintain satisfactory performance at small angles of attack. Without the gap, air distortion was large and pressure recovery was low.
2. A properly designed shield, such as that for the large model, could reduce distortion appreciably at angle of attack. With the large model, distortion was reduced by half at an angle of attack of  $8^{\circ}$ . The shield on the small model increased distortion at all angles of attack below  $12^{\circ}$ , and this configuration had the least distortion at an angle of attack of  $14^{\circ}$ .
3. The shields improved subcritical stability at angle of attack. Pivoting the cone of the small model with the shield in position produced further improvements in stability.

Lewis Flight Propulsion Laboratory  
National Advisory Committee for Aeronautics  
Cleveland, Ohio, August 9, 1957

## REFERENCES

1. Perchonok, Eugene, Wilcox, Fred, and Pennington, Donald: Effect of Angle of Attack and Exit Nozzle Design on the Performance of a 16-Inch Ram Jet at Mach Numbers from 1.5 to 2.0. NACA RM E51G26, 1951.
2. Leissler, L. Abbott, and Hearth, Donald P.: Preliminary Investigation of Effect of Angle of Attack on Pressure Recovery and Stability Characteristics for a Vertical-Wedge-Nose Inlet at Mach Number of 1.90. NACA RM E52E14, 1952.

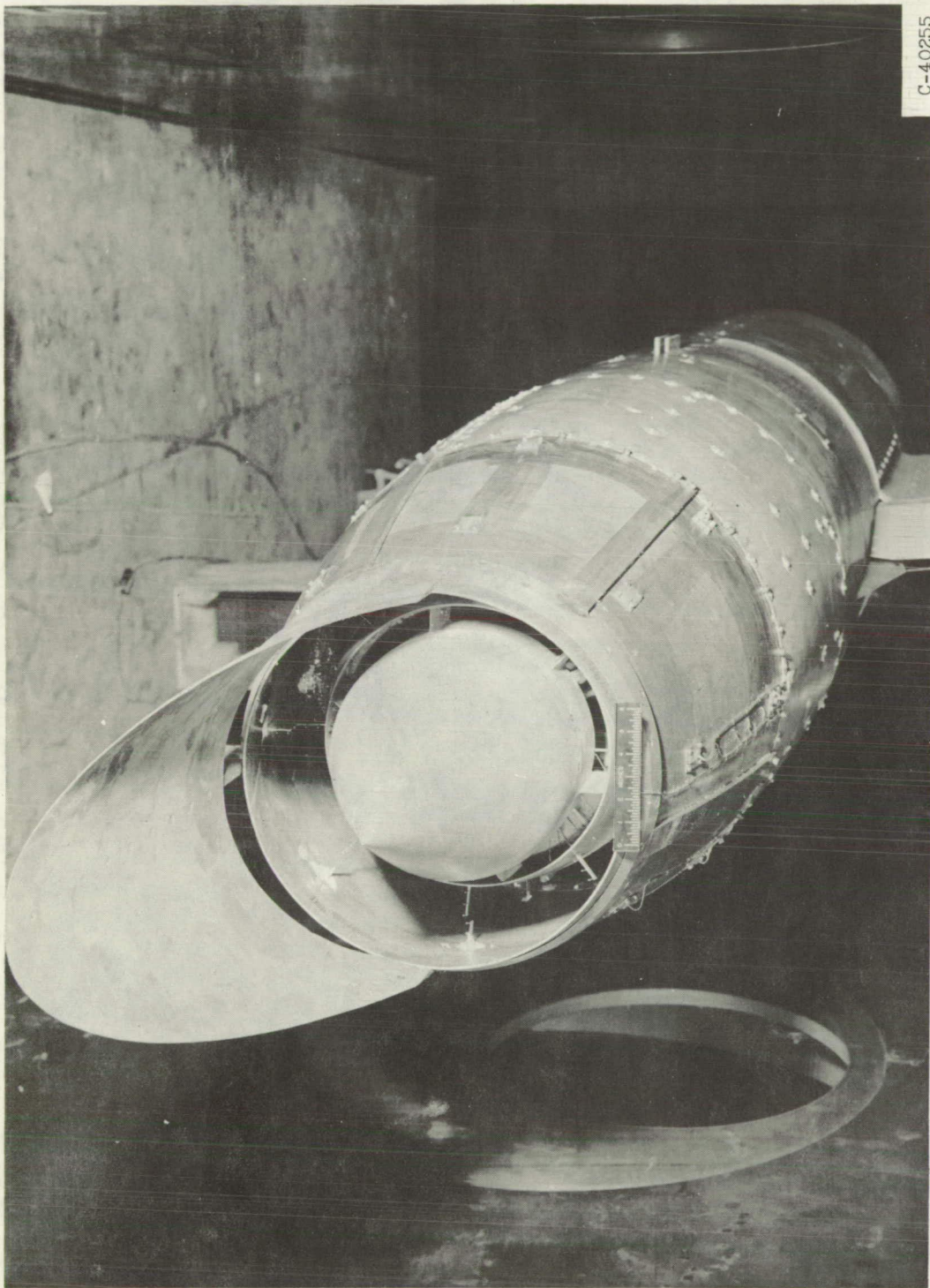
3. Beheim, Milton A.: A Preliminary Investigation at Mach Number 1.91 of an Inlet Configuration Designed for Insensitivity to Positive Angle-of-Attack Operation. NACA RM E53E20, 1953.
4. Beheim, Milton A.: A Preliminary Investigation at Mach Number 1.91 of a Diffuser Employing a Pivoted Cone to Improve Operation at Angle of Attack. NACA RM E53I30, 1953.
5. Schueller, Carl F., and Stitt, Leonard E.: An Inlet Design Concept to Reduce Flow Distortion at Angle of Attack. NACA RM E56K28b, 1957.
6. Piercy, Thomas G., and Chiccine, Bruce G.: Development of Flow Distortions in a Full-Scale Nacelle Inlet at Mach Numbers 0.63 and 1.6 to 2.0. NACA RM E56G13a, 1956.



(a) Large-scale model, side view.

Figure 1. - Photographs of models.

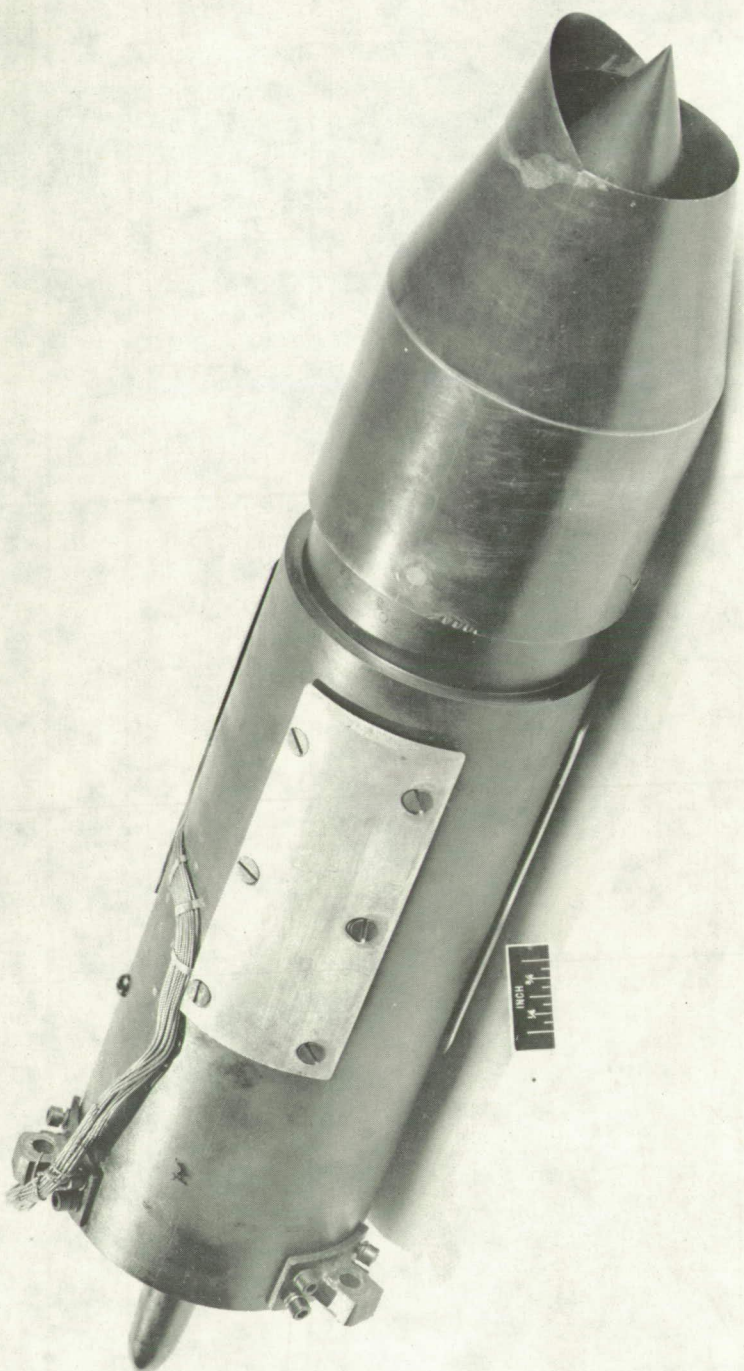
C-40255



(b) Large-scale model, front view.

Figure 1. - Continued. Photographs of models.

C-33286



(c) Small-scale model.

Figure 1. - Concluded. Photographs of models.

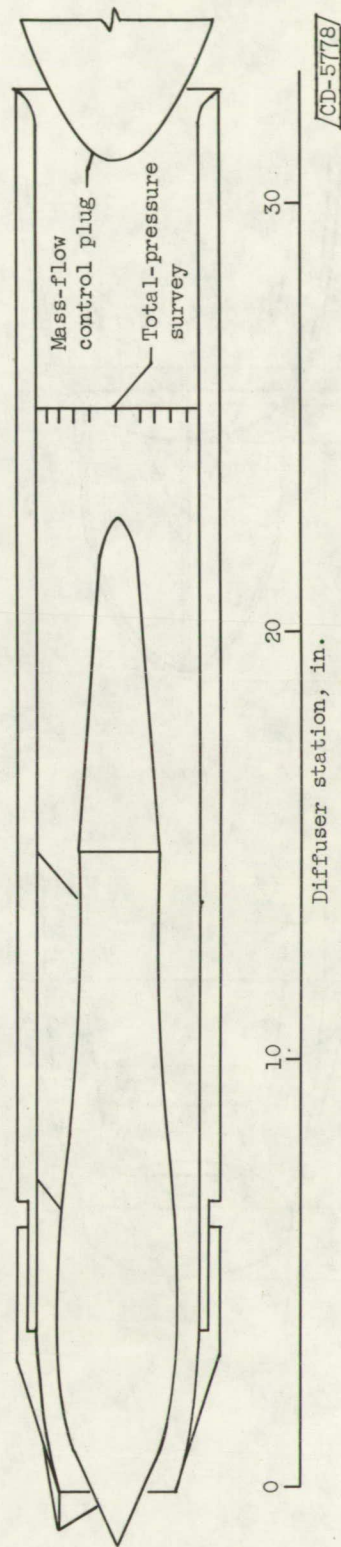
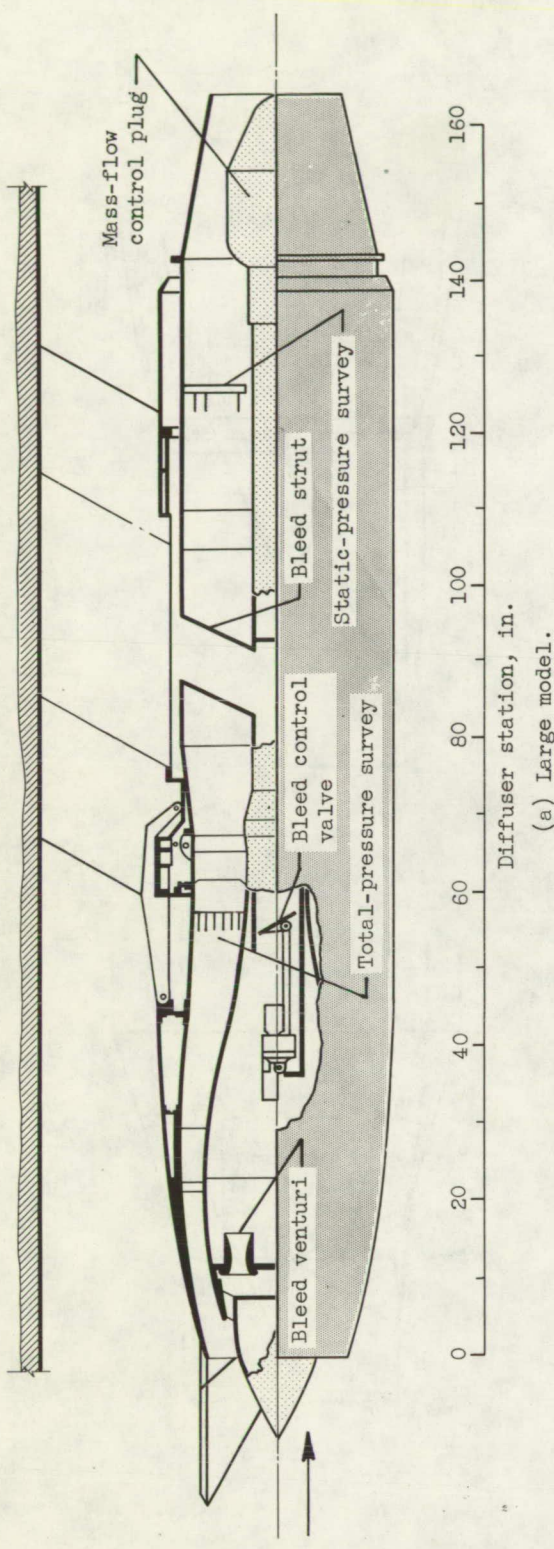
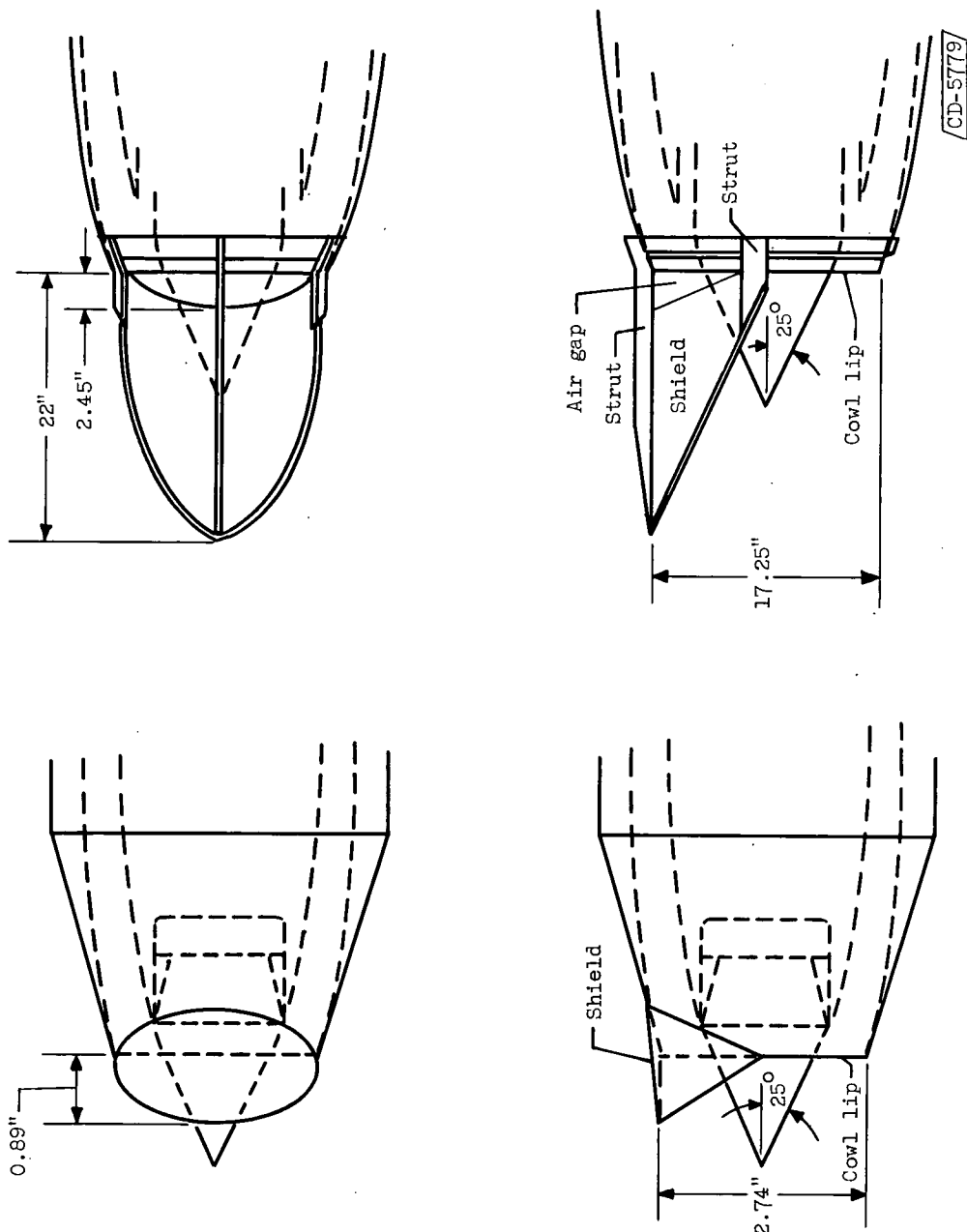


Figure 2. - Schematic sketches of inlets.



(d) Large-shield detail.

Figure 2. - Concluded. Schematic sketches of inlets.

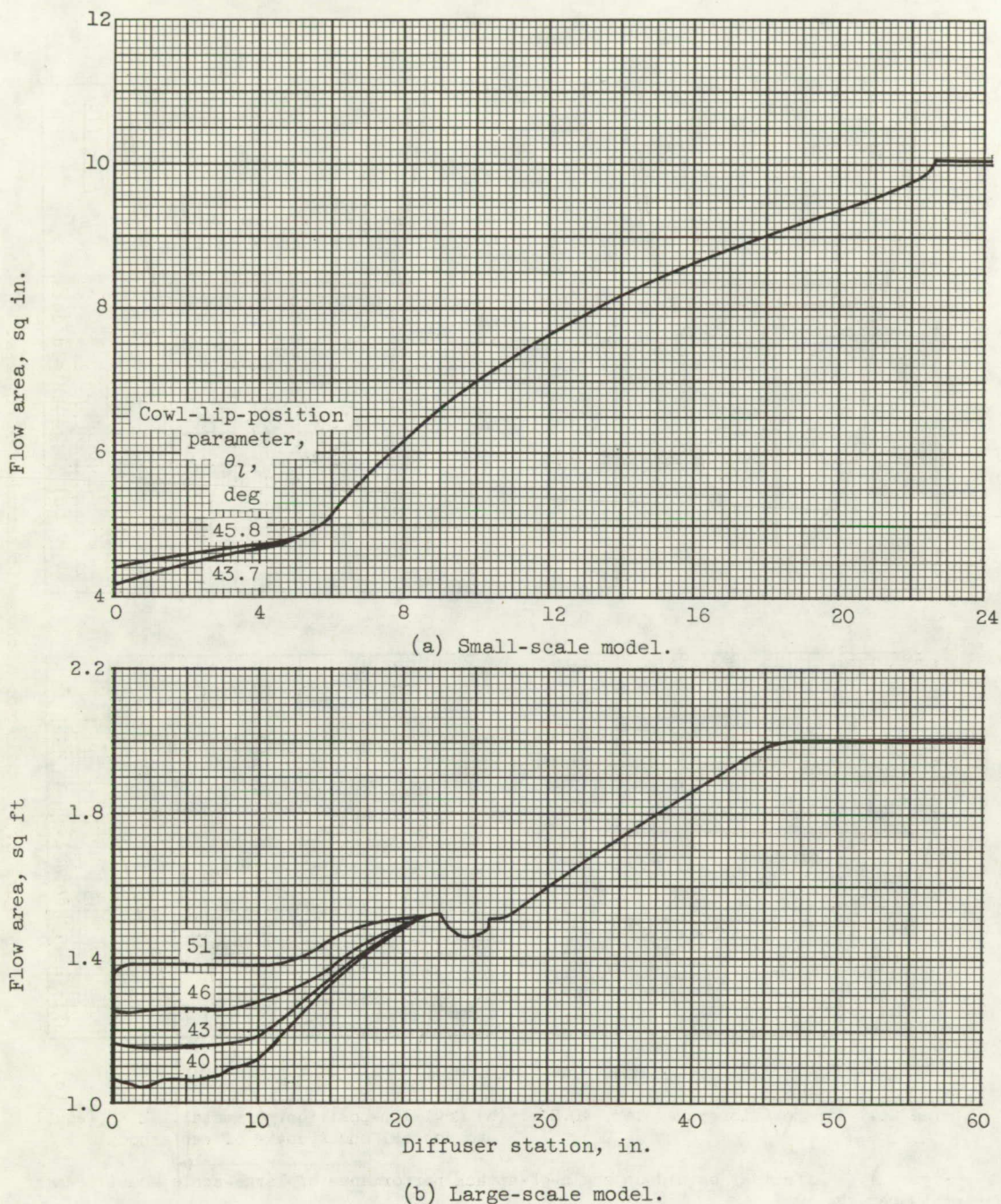
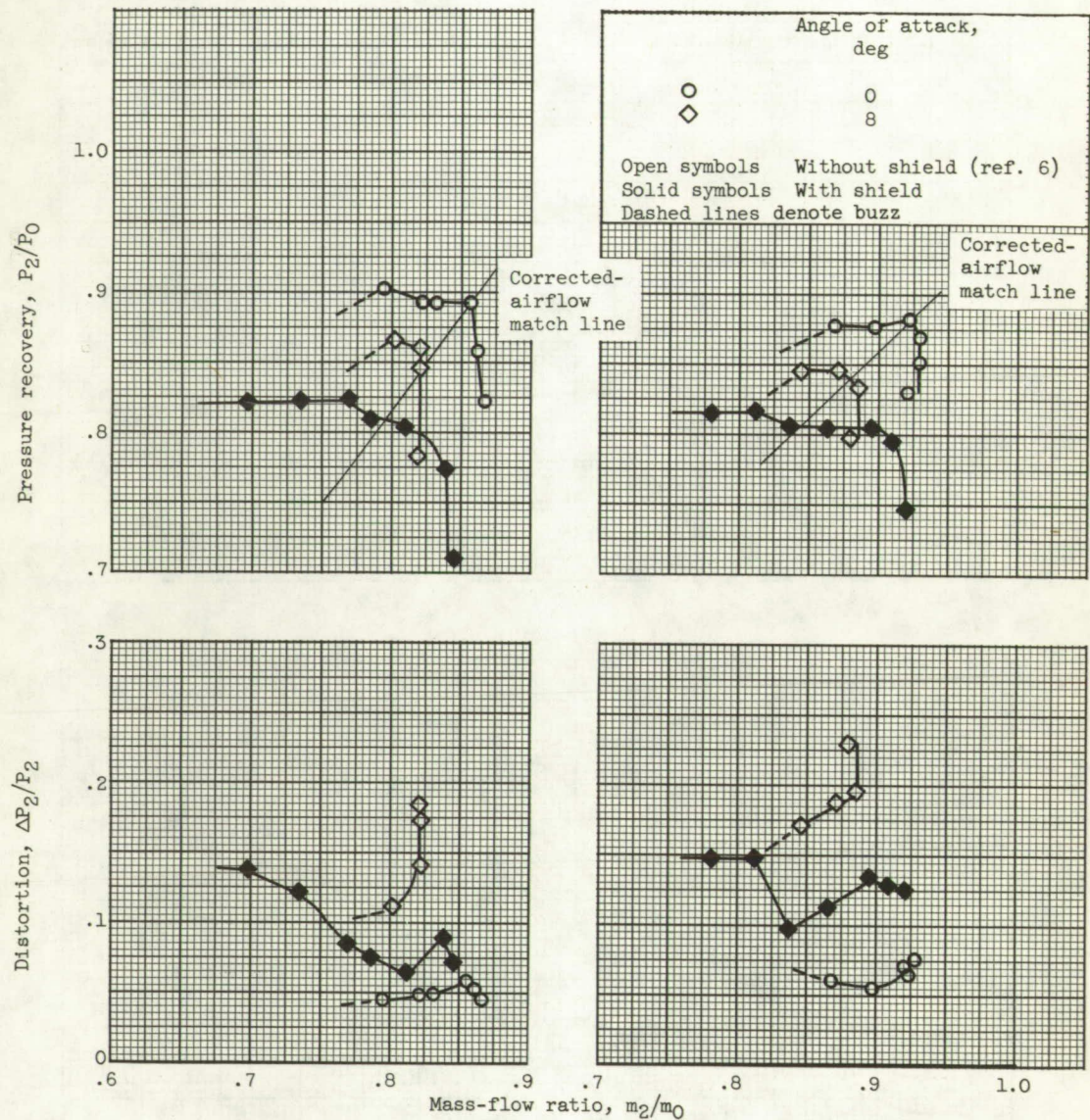


Figure 3. - Diffuser area variations.



(a) Cowl-lip-position parameter,  $40.0^\circ$ . (b) Cowl-lip-position parameter,  $42.6^\circ$  (equal to conical shock angle of centerbody).

Figure 4. - Effect of shield on angle-of-attack performance of large-scale model. Mach number, 2.

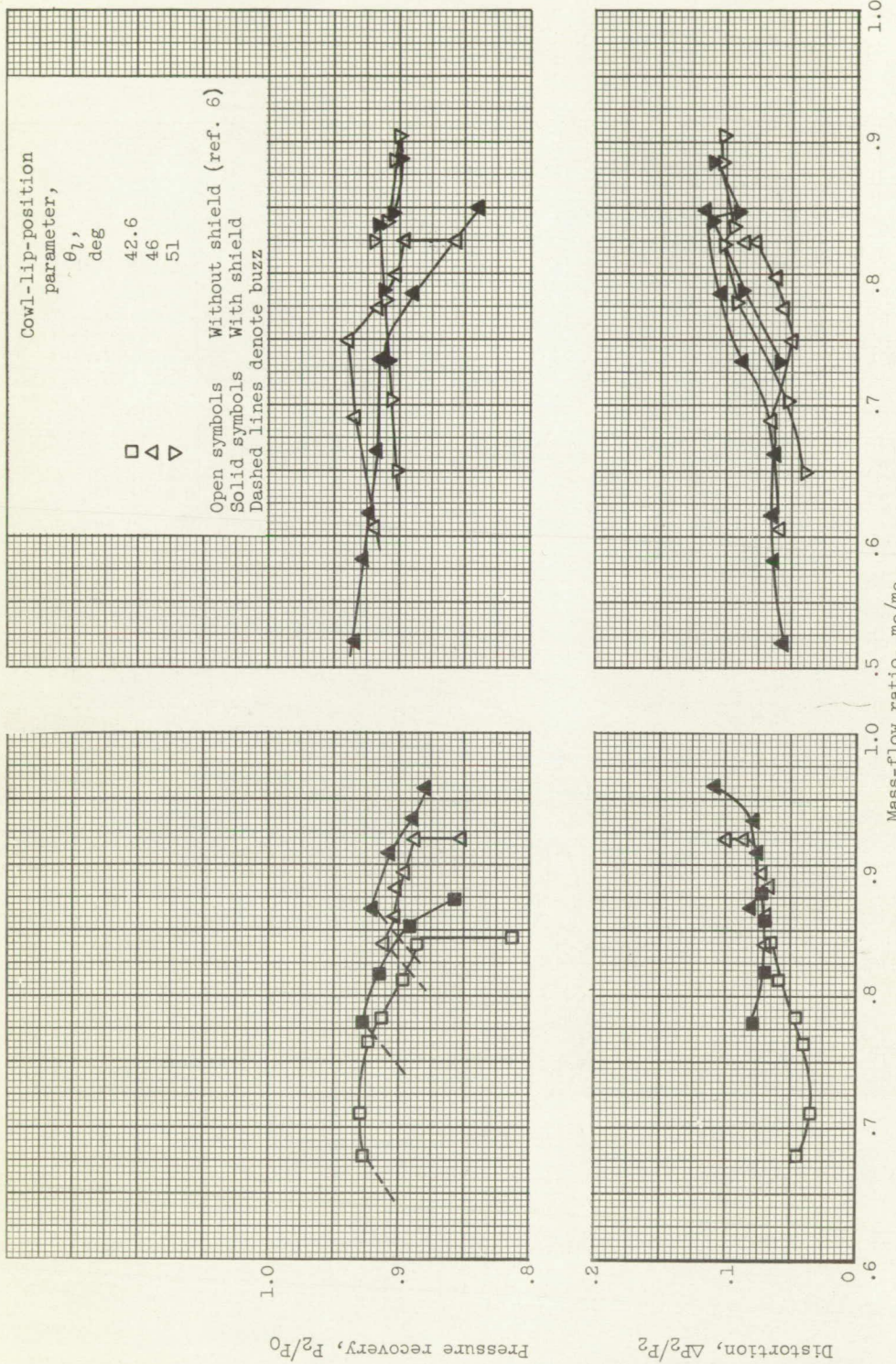
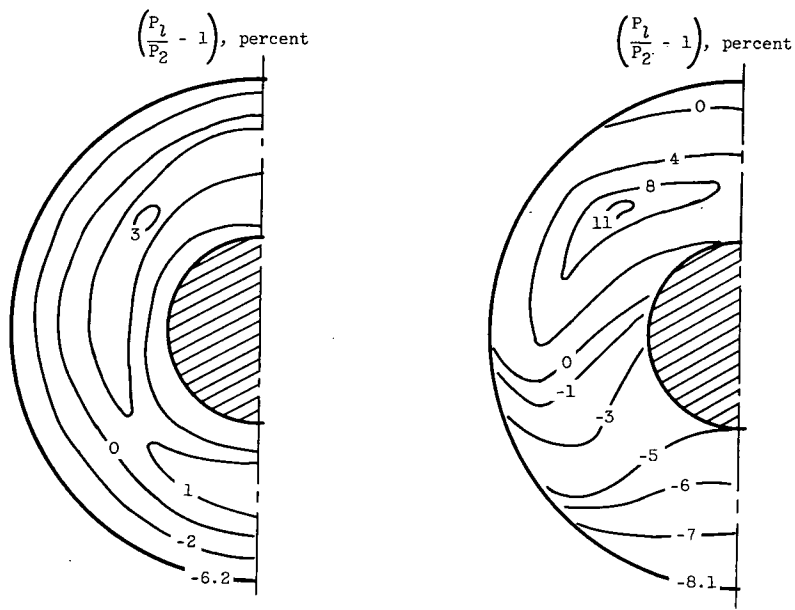
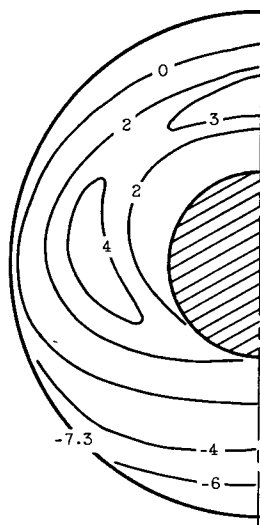


Figure 5. - Effect of shield on zero-angle-of-attack performance of large-scale model.



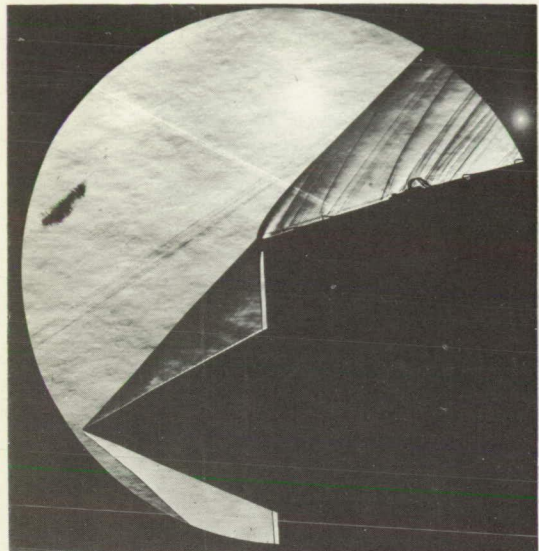
(a) Angle of attack, zero;  
without shield; mass-  
flow ratio, 0.922; pres-  
sure recovery, 0.881;  
distortion, 0.065.

(b) Angle of attack, 8°;  
without shield; mass-  
flow ratio, 0.869; pres-  
sure recovery, 0.845;  
distortion, 0.188.

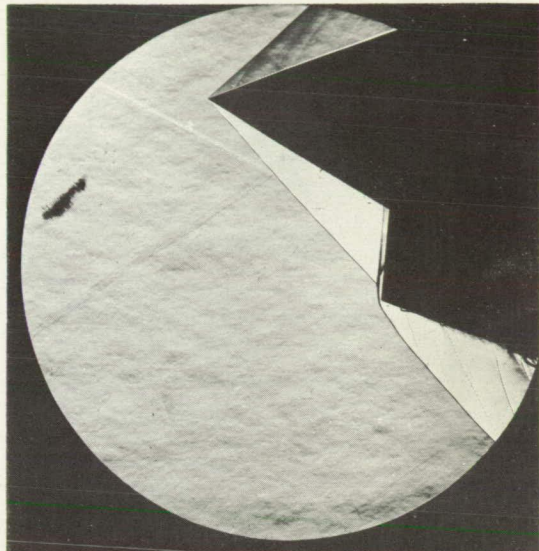
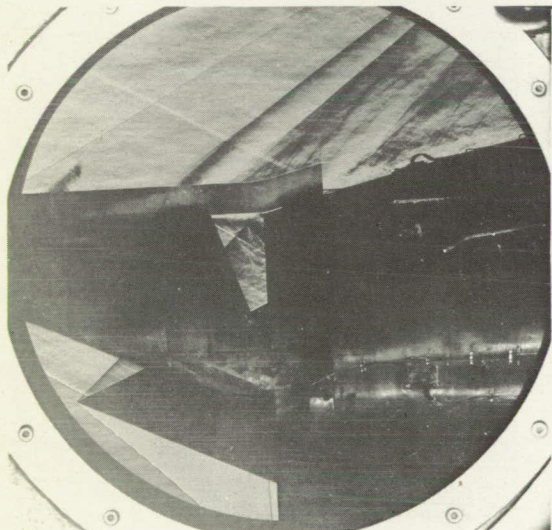


(c) Angle of attack, 8°;  
with shield (located  
on upper half); mass-  
flow ratio, 0.895;  
pressure recovery,  
0.805; distortion,  
0.129.

Figure 6. - Distortion contours at diffuser exit (station 58) of large-scale model. Critical operation; Mach number, 2.  $P_l$  and  $P_2$ : local and diffuser-exit total pressures, respectively.



(a) Without shield; angle of attack, zero.

(b) Without shield; angle of attack,  $8^\circ$ .

(c) With shield; angle of attack, zero.

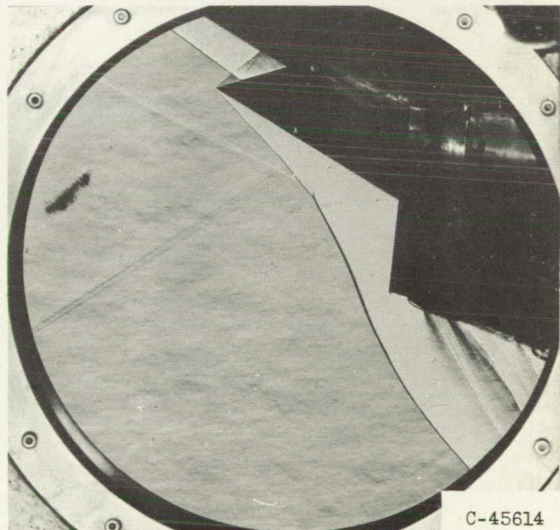
(d) With shield; angle of attack,  $8^\circ$ .

Figure 7. - Schlieren photographs of large-scale model. Supercritical operation; Mach number, 2; cowl-lip-position parameter,  $42.6^\circ$ .

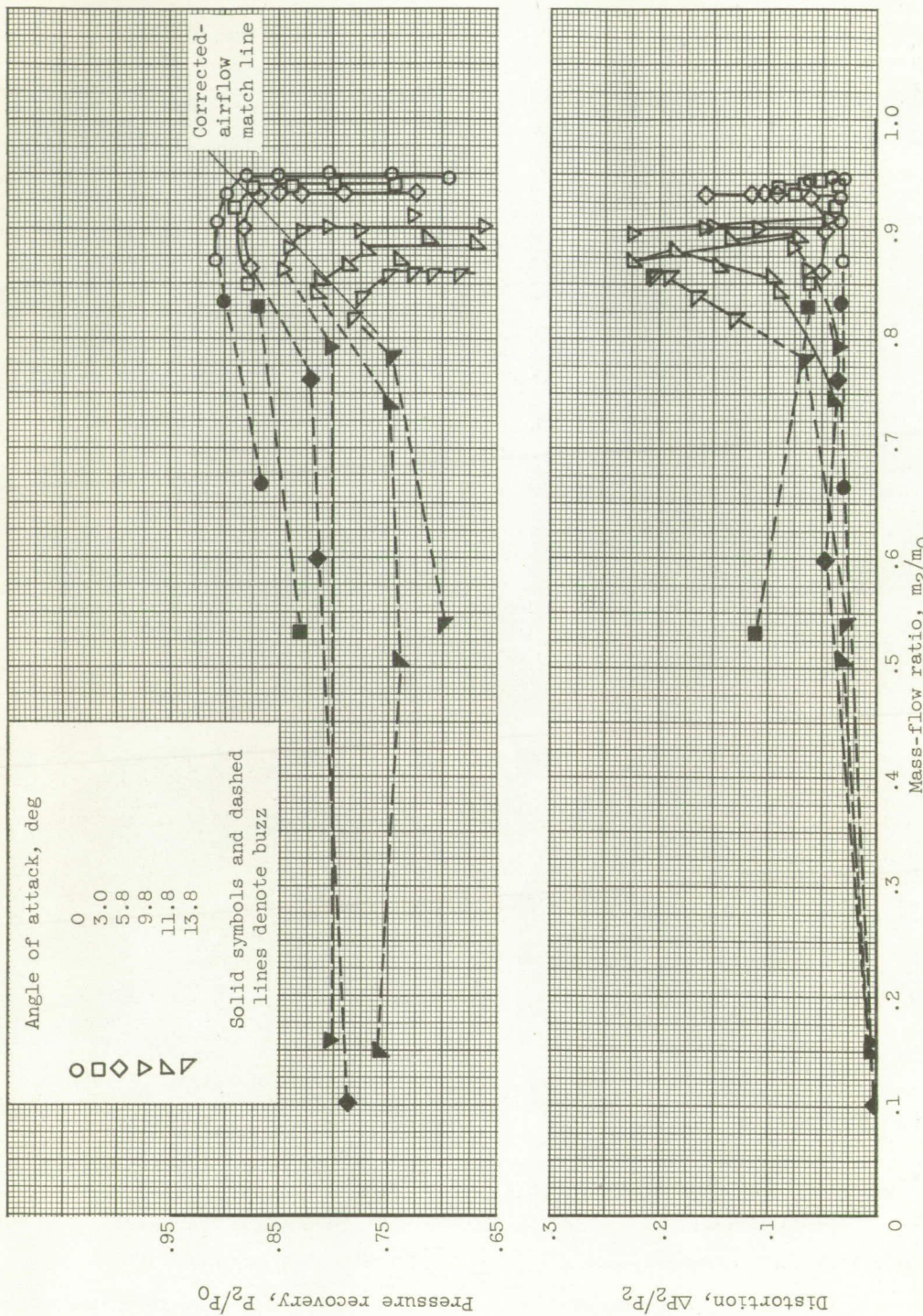
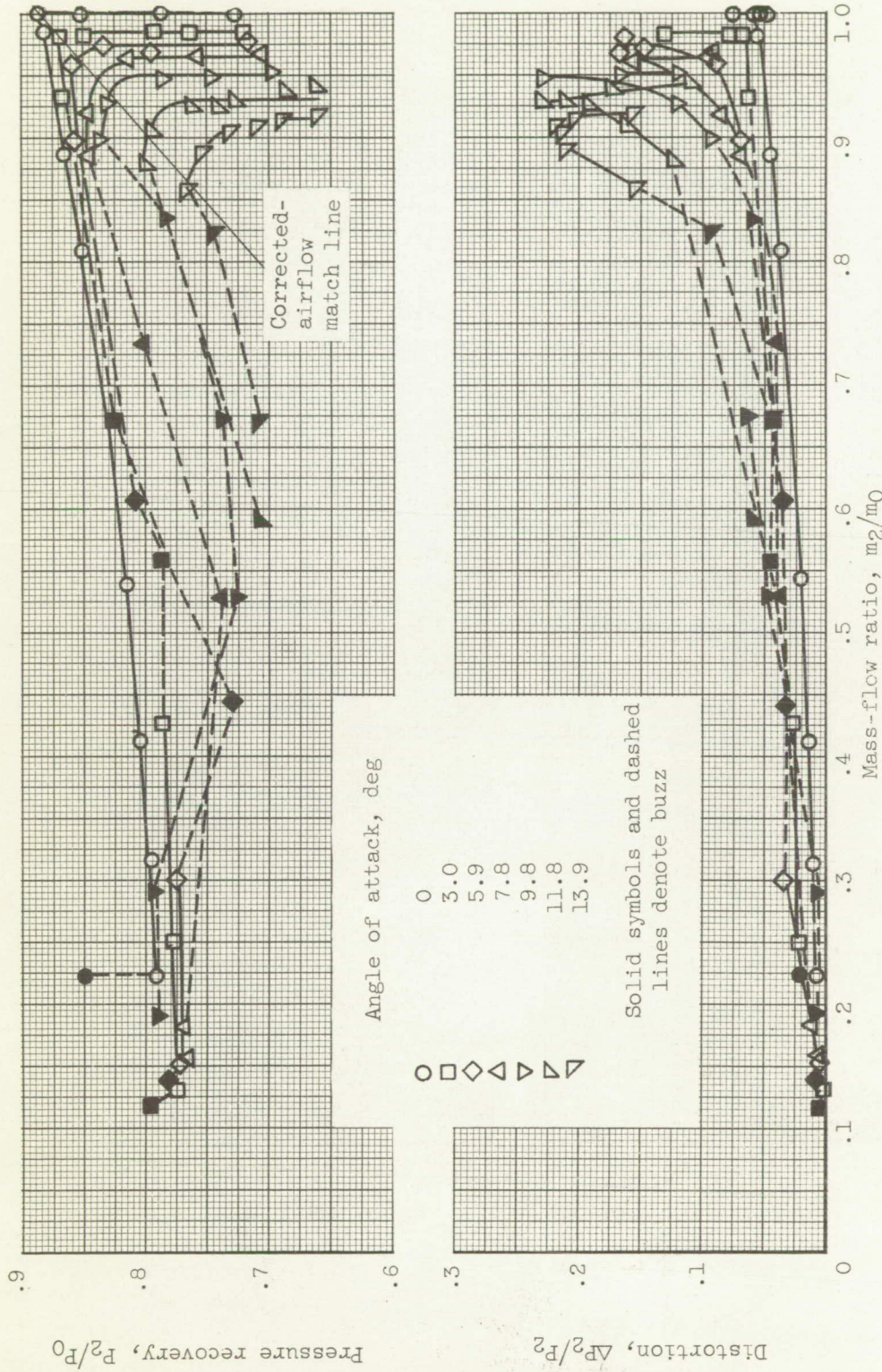


Figure 8. - Angle-of-attack performance of small-scale model without shield. Mach number, 1.91.



(b) Cowl-lip-position parameter,  $44.7^\circ$ .  
Figure 8. - Concluded. Angle-of-attack performance of small-scale model without shield. Mach number, 1.91.

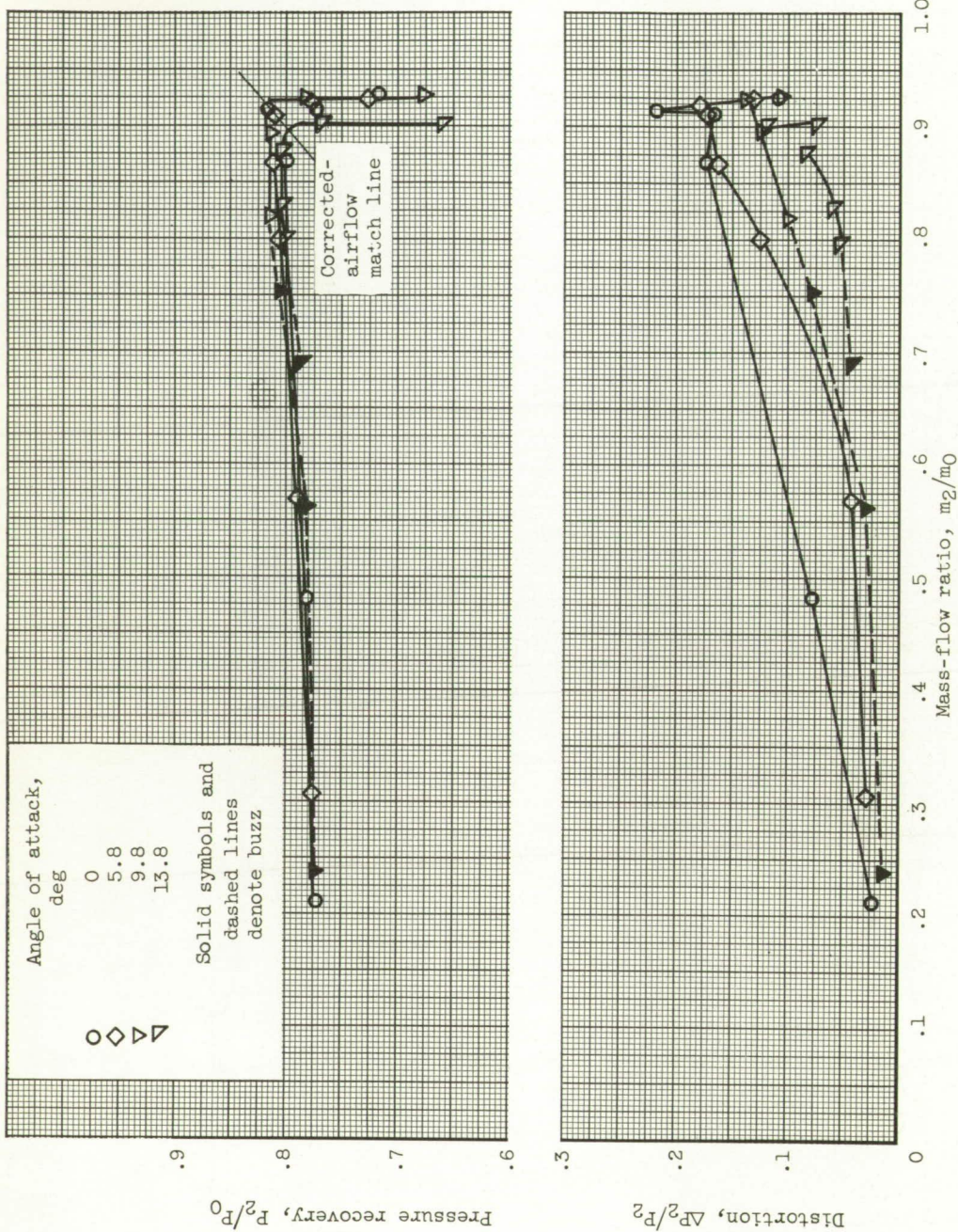
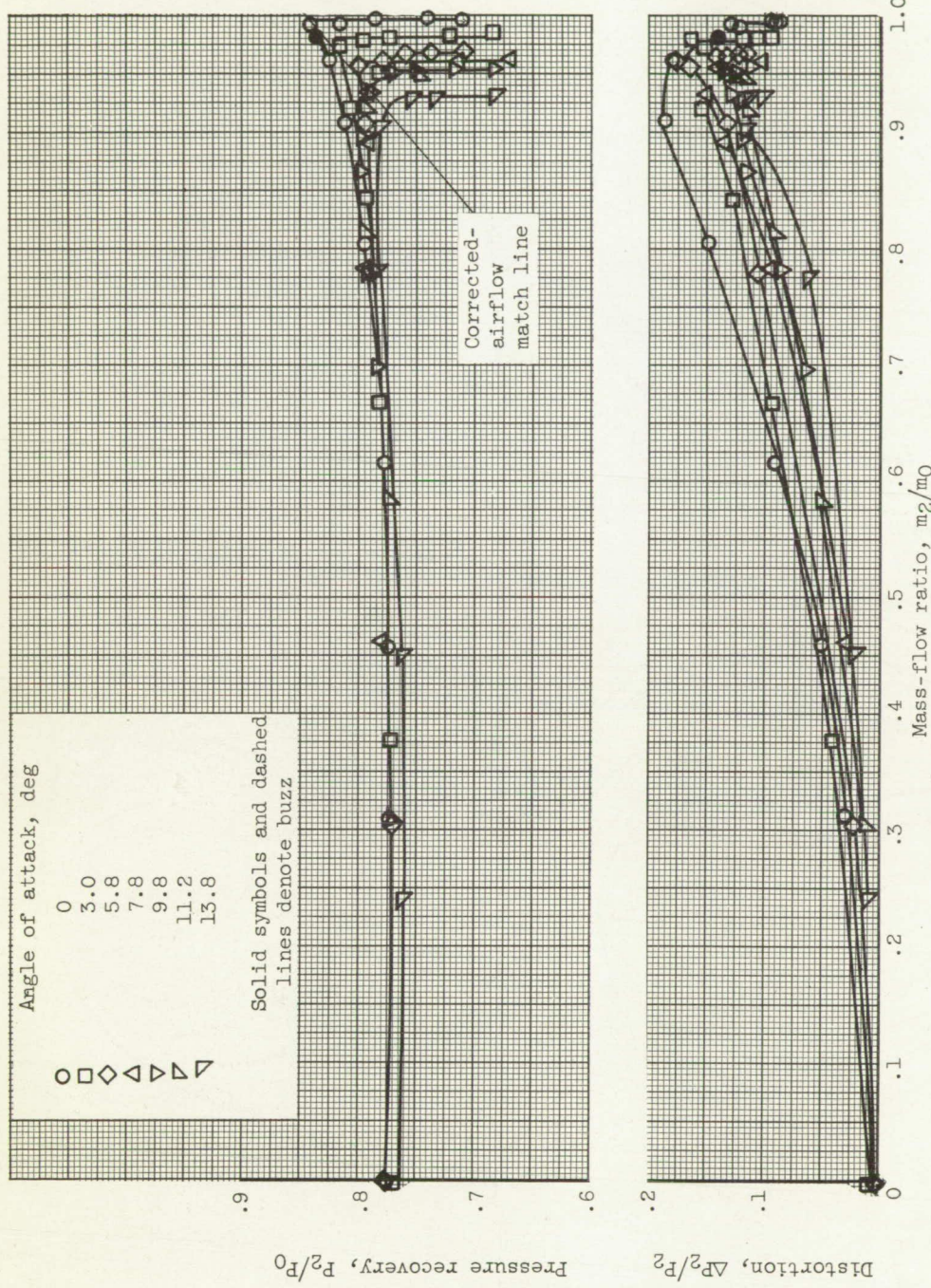
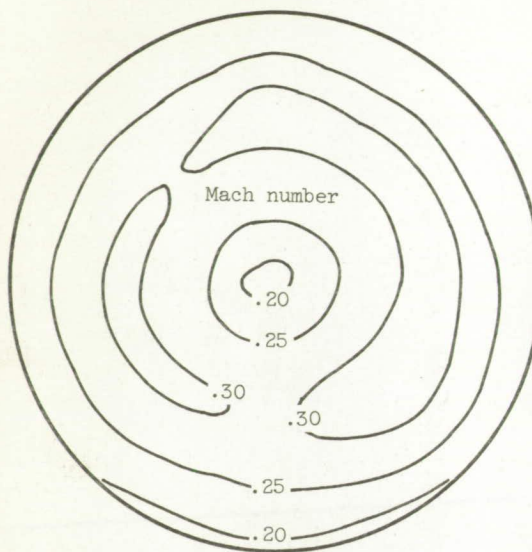
(a) Cowl-lip-position parameter,  $41.8^\circ$ .

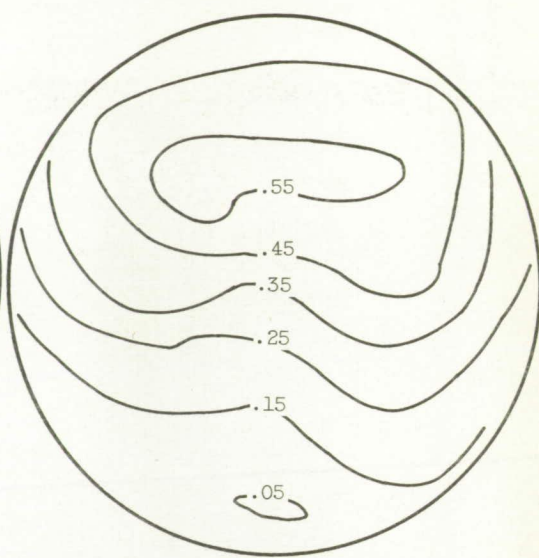
Figure 9. - Angle-of-attack performance of small-scale model with shield. Mach number, 1.91.



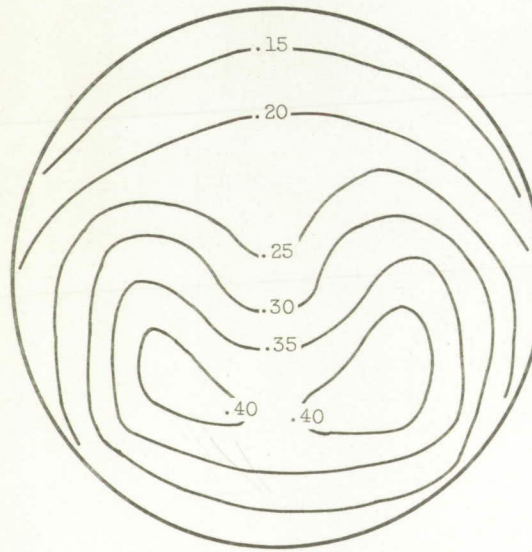
(b) Cowl-lip-position parameter,  $44.7^\circ$ .  
 Figure 9. - Concluded. Angle-of-attack performance of small-scale model with shield. Mach number, 1.91.



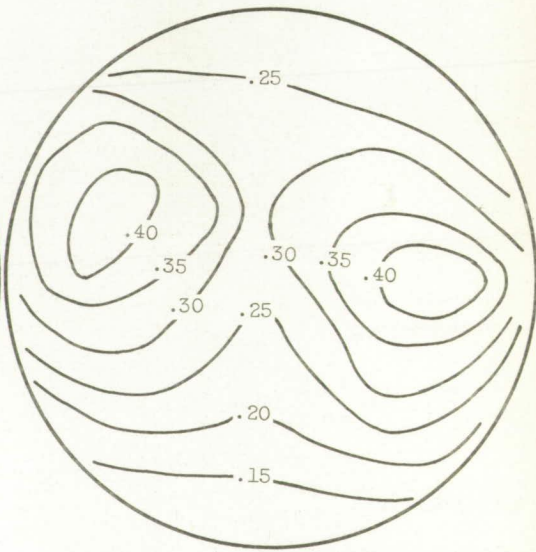
(a) Angle of attack, zero; without shield; mass-flow ratio, 1.00; pressure recovery, 0.884; distortion, 0.045.



(b) Angle of attack, 14°; without shield; mass-flow ratio, 0.908; pressure recovery, 0.706; distortion, 0.218.

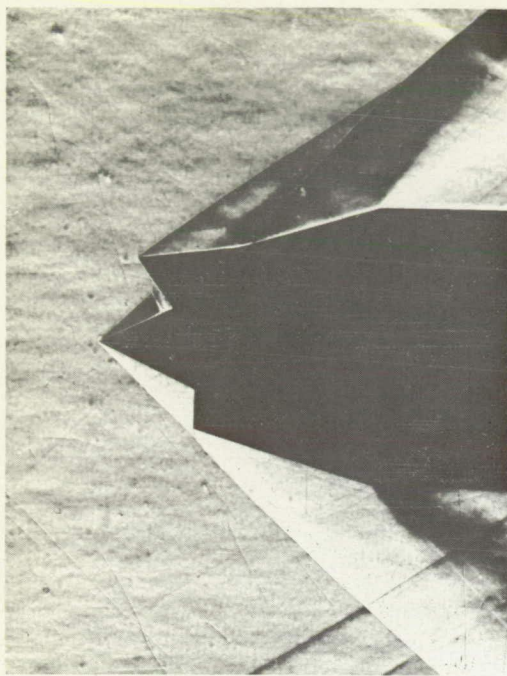


(c) Angle of attack, zero; with shield (located on upper half); mass-flow ratio, 0.992; pressure recovery, 0.839; distortion, 0.086.

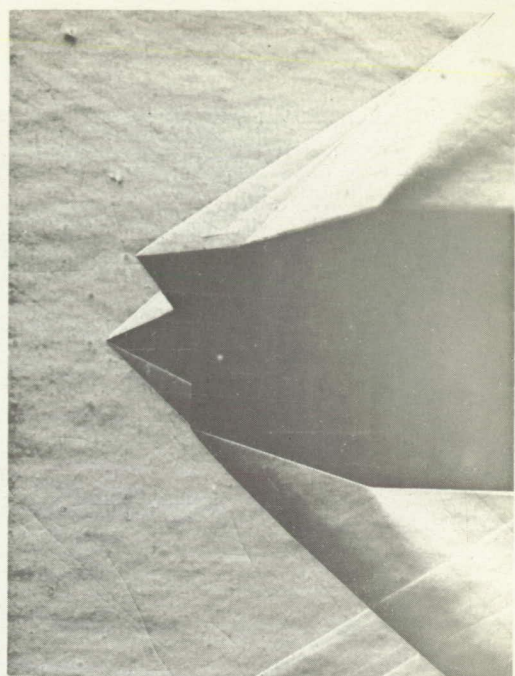


(d) Angle of attack, 14°; with shield (located on upper half); mass-flow ratio, 0.930; pressure recovery, 0.754; distortion, 0.119.

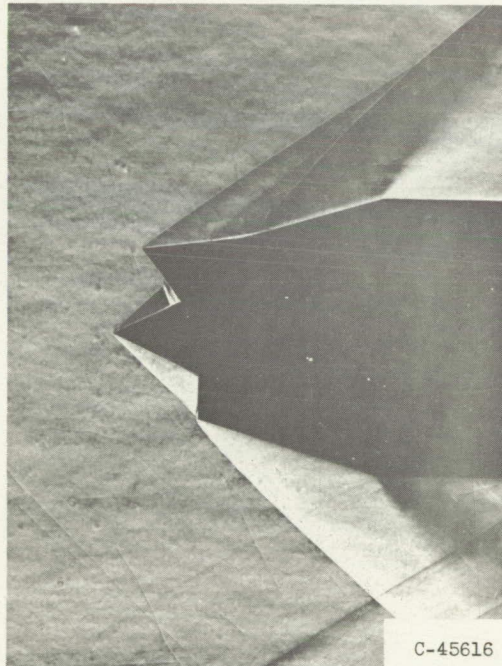
Figure 10. - Effect of shield on Mach number contours at exit of small-scale model. Cowl-lip-position parameter, 44.7°; critical operation; Mach number, 1.91.



(a) Angle of attack, zero; cowl-lip-position parameter,  $41.8^\circ$ ; super-critical operation.



(b) Angle of attack, zero; cowl-lip-position parameter,  $44.7^\circ$ ; super-critical operation

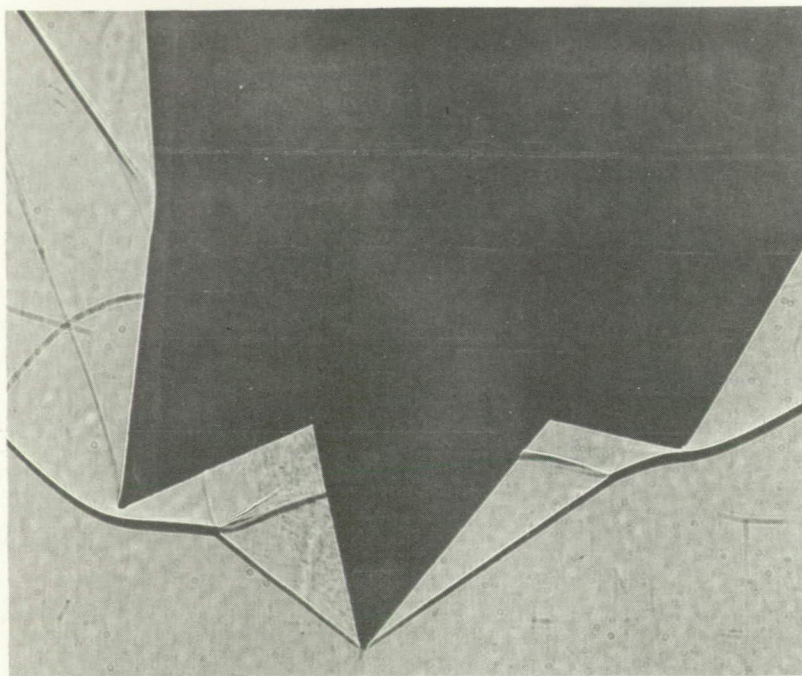


C-45616

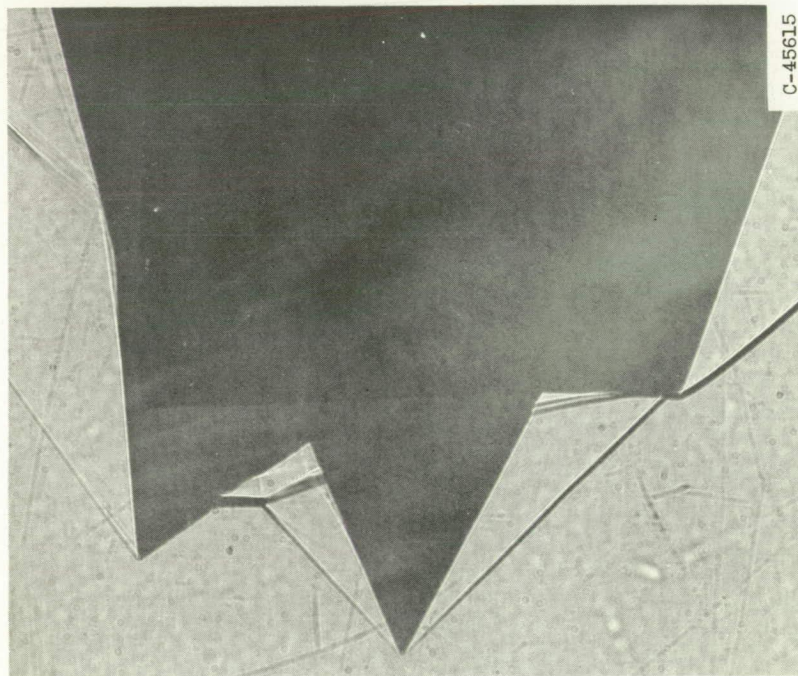
(c) Angle of attack, zero; cowl-lip-position parameter,  $44.7^\circ$ ; subcritical operation, buzz just stopped.

Figure 11. - Schlieren and shadowgraph photographs of small-scale model. Mach number, 1.91.

CONFIDENTIAL



(e) Angle of attack,  $14^\circ$ ; cowl-lip-position parameter,  $44.7^\circ$ ; supercritical operation.



(d) Angle of attack,  $3^\circ$ ; cowl-lip-position parameter,  $44.7^\circ$ ; supercritical operation.

Figure 11. - Concluded. Schlieren and shadowgraph photographs of small-scale model.  
Mach number, 1.91.

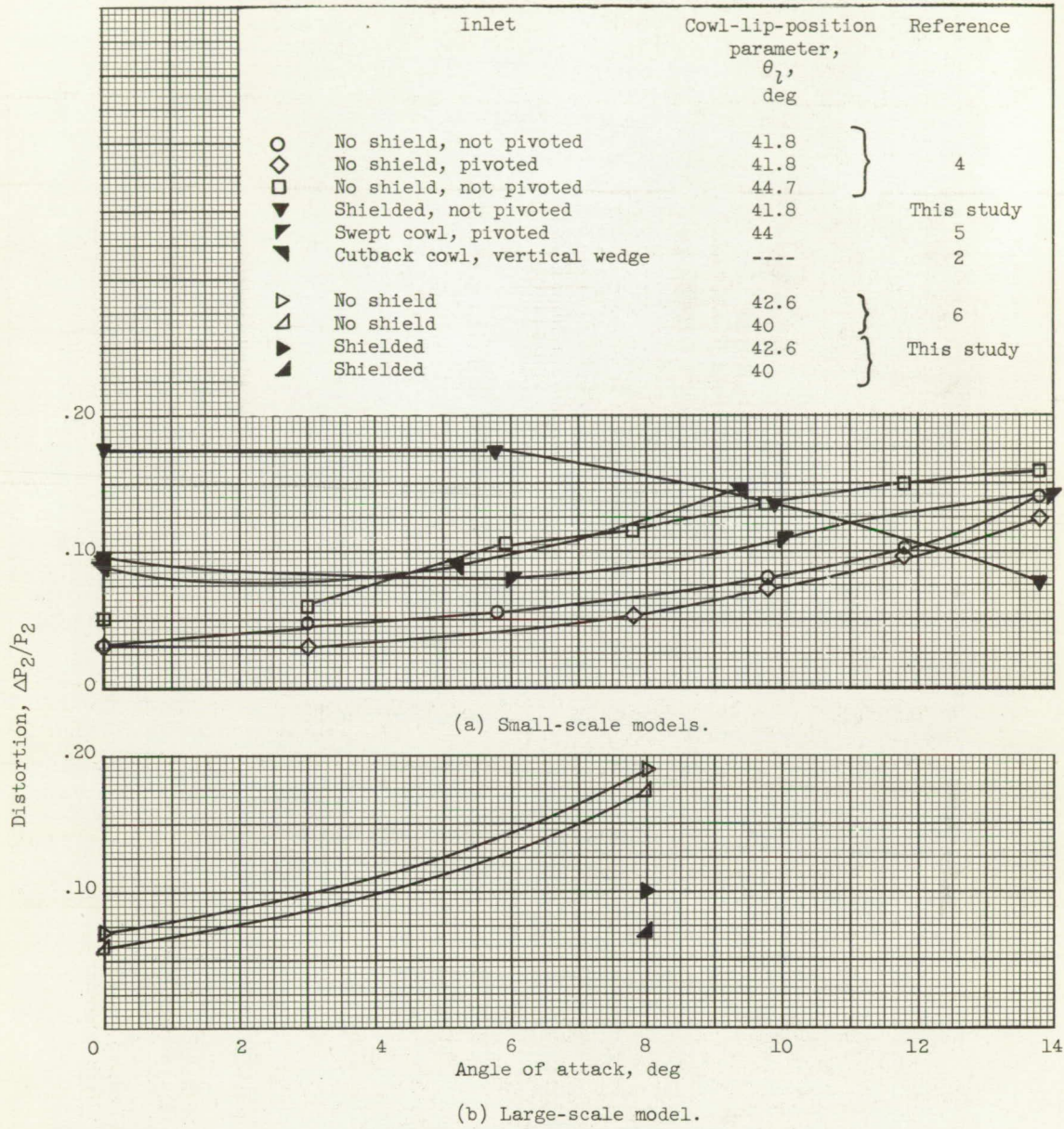


Figure 12. - Comparison of distortion over angle-of-attack range for several inlets for constant diffuser-exit Mach number.

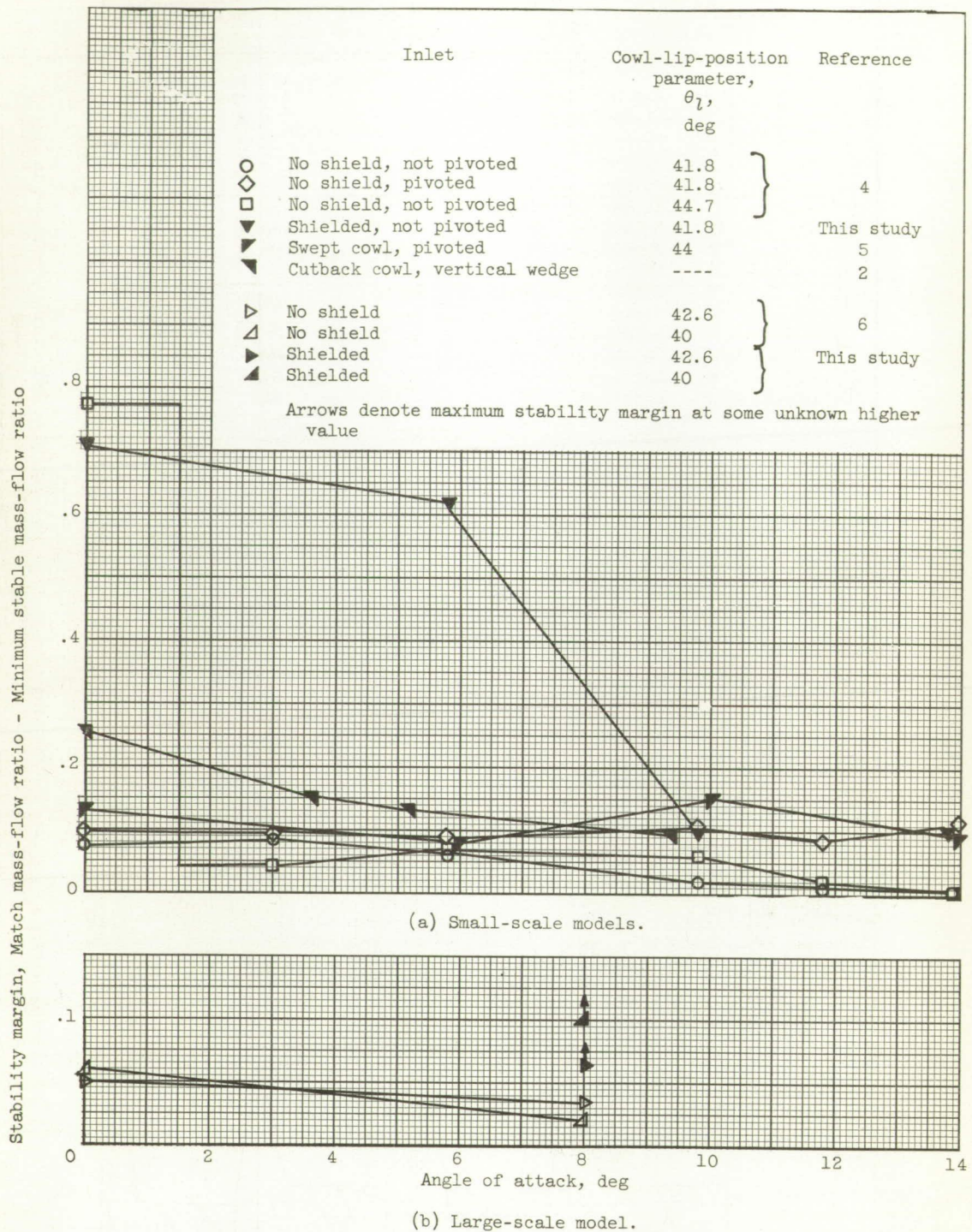
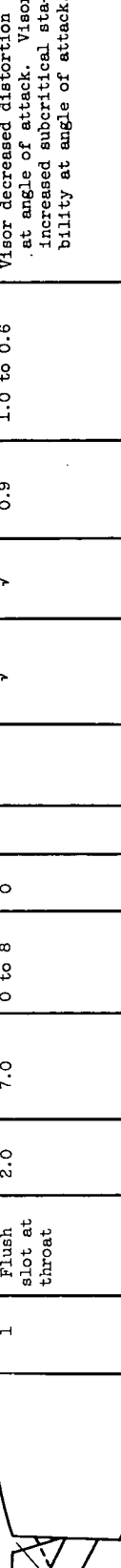
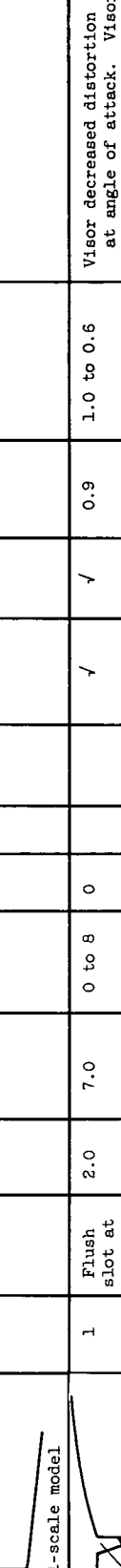
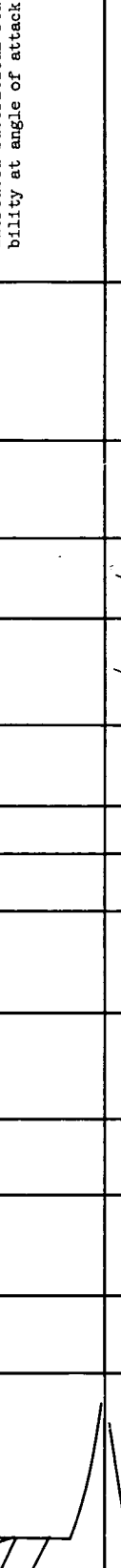
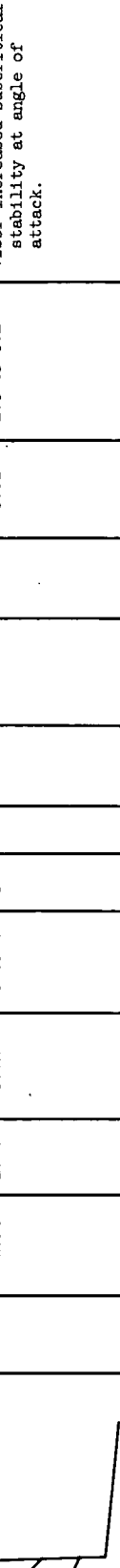


Figure 13. - Comparison of stability margin over angle-of-attack range for several inlets for constant diffuser-exit Mach number.

NOTES: (1) Reynolds number is based on the diameter of a circle with the same area as that of the capture area of the inlet.

(2) The symbol \* denotes the occurrence of buzz.

Report and facility	Description	Test parameters				Test data			Performance		Remarks	
		Number of oblique shocks	Type of boundary-layer control	Reynolds number $\times 10^6$	Angle of attack, deg	Angle of yaw, deg	Drag	Inlet flow profile	Discharge-flow profile	Flow picture	Maximum total-pressure recovery	
CONFID. RM E57G25a Lewis 8- by 6-foot supersonic wind tunnel		1	Flush slot at throat	2.0	7.0	0 to 8	0			/	0.9	1.0 to 0.6
CONFID. RM E57G25a Lewis 18- by 18-inch Mach 1.9 wind tunnel		1	None	1.91	0.71	0 to 14	0			/	0.82	1.0 to 0.1
CONFID. RM E57G25a Lewis 8- by 6-foot supersonic wind tunnel		1	Flush slot at throat	2.0	7.0	0 to 8	0			/	0.9	1.0 to 0.6
CONFID. RM E57G25a Lewis 18- by 18-inch Mach 1.9 wind tunnel		1	None	1.91	0.71	0 to 14	0			/	0.82	1.0 to 0.1

#### Bibliography

These strips are provided for the convenience of the reader and can be removed from this report to compile a bibliography of NACA inlet reports. This page is being added only to inlet reports and is on a trial basis.

CONFIDENTIAL

~~CONFIDENTIAL~~

**UNCLASSIFIED**

TECHNICAL LIBRARY  
AIRSEARCH MANUFACTURING CO.  
9851-9951 SEPULVEDA BLVD.  
LOS ANGELES 45

CALIFORNIA

**UNCLASSIFIED**

~~CONFIDENTIAL~~